JACS
JOURNAL OF THE AMERICAN CHEMICAL SOCIETY

Communication

pubs.acs.org/JACS

# Selective Growth of Dual-Color-Emitting Heterogeneous Microdumbbells Composed of Organic Charge-Transfer Complexes

Yi Long Lei, Liang Sheng Liao,* and Shuit Tong Lee*

Jiangsu Key Laboratory for Carbon-Based Functional Materials and Devices, Institute of Functional Nano and Soft Materials (FUNSOM), Soochow University, Suzhou, Jiangsu 215123, China

Supporting Information

**ABSTRACT:** We report a simple yet versatile solution route for constructing heterojunctions from luminescent organic charge-transfer (CT) complexes through a two-step seeded-growth method. Using this method, we achieved anisotropic and selective growth of anthracene−1,2,4,5-tetracyanobenzene (TCNB) complexes onto the tips of naphthalene−TCNB microtubes, resulting in the formation of microdumbbells. Significantly, the two-component microdumbbells appear as dual-color-emitting heterojunctions arising from integration of two distinct color-emitting materials. We further elucidated the two-step seeded-growth mechanism of the dumbbell-like organic heterostructures on the basis of structural analysis of the two crystals and surface−interface energy balance. In principle, the present synthetic route may be used to fabricate a wide range of sophisticated dual- or multicolor-emitting organic heterostructures via judicious choice of the CT complexes.

Heterostructured nanomaterials with desirable spatial organization of diverse materials are being designed and constructed to meet ever-increasing technological requirements.[1] Multifunctional lab-on-a-particle architectures have demonstrated that the creation of proper interfaces between dissimilar constituent domains can lead to remarkable performance improvement due to synergistic effects of the individual components. A representative example is the case of Au nanocrystals selectively grown onto CdS nanorods to form matchstick- or dumbbell-like hybrid nanostructures,[1f,2] which yielded dramatic fluorescence quenching due to light-induced charge separation at the metal−semiconductor interface. In addition to unique optical properties, heterostructured nanomaterials also exhibit exciting potential in different applications, such as magnetism,[3] medical diagnostics,[4] and photocatalysis.[5] Consequently, extensive efforts have been directed toward the controlled synthesis of inorganic heterostructured nanomaterials. Fabrication of inorganic heterostructures has been commonly performed via selective growth of metal or semiconductor nanoparticles onto the tips of existing metal chalcogenide seed nanorods.[1d−h,2,3] Similarly, organic heterostructured micro- and nanomaterials are particularly attractive in view of the diversity of organic materials and their wide-ranging functional properties. However, the controlled synthesis of organic heterostructures has been rare and remains a difficult challenge, in contrast to that of their inorganic counterparts. Recently, segmented nanotubular heterojunctions made of graphite-like organic molecules with dissimilar semiconducting properties were synthesized by liquid-phase stepwise coassembly.[6] Also, heterojunctioned nanoribbons were formed from copper phthalocyanine and its fluorinated counterpart.[7] Such integration of organic molecules to realize lab-on-a-particle architectures represents a rapidly advancing field of research. However, the lack of understanding and control of molecular self-assembly has severely hampered the development of organic multicomponent heterostructures.

Here we report a facile two-step seeded-growth process for the fabrication of microtubular heterojunctions of organic charge-transfer (CT) complexes. This process involves selective nucleation and growth of secondary CT complexes onto specific facets of well-dispersed CT complex microtubes used as seeds. The proper concentration of the secondary component must be used to avoid homogeneous nucleation in the stepwise coassembly process. The strong solid-state emission of CT complexes[8,9] allowed us demonstrate the efficacy of the two-step seeded-growth process by fabricating dual-color-emitting heterostructures via integration of two distinct crystalline luminescent CT complexes. To exemplify the process, anisotropic naphthalene−1,2,4,5-tetracyanobenzene (TCNB) microtubes[9] were used as seeds, and selective nucleation and growth of a secondary material, anthracene−TCNB, onto the tips of the seeds formed so-called "microdumbbells". Significantly, the heterostructured microdumbbells yielded strong dual-color heterogeneous emission due to the distinct solid-state luminescence of naphthalene−TCNB and anthracene−TCNB. The two-step seeded-growth mechanism of the dumbbell-like organic heterostructures was elucidated through structural analysis of the two crystals and surface−interface energy balance. As a new and exciting model material, these organic luminescent microdumbbells offer important insights into the selective nucleation and growth of CT complexes that may prove useful in novel optoelectronic devices.

We selected naphthalene−TCNB and anthracene−TCNB (Figure 1a) as the model compounds because of their chemical and structural compatibility. Scanning electron microscopy (SEM) (Figure 1b) revealed that the naphthalene−TCNB seed microtubes were successfully prepared via etching-assisted CT-induced self-assembly, as reported previously.[9] The 1D tubular structures were formed with a rectangular cross section, a fairly uniform diameter of 3 $\mu$m, and lengths of hundreds of

**Received:** November 21, 2012
**Published:** March 4, 2013





dx.doi.org/10.1021/ja3114278 | J. Am. Chem. Soc. 2013, 135, 3744−3747

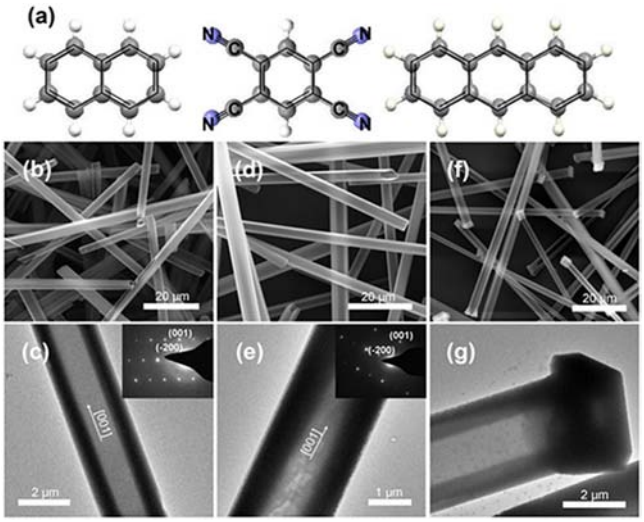


**Figure 1.** (a) Schematic showing the molecular structures of (left to right) naphthalene, TCNB, and anthracene. (b, d, f) SEM images showing (b) naphthalene−TCNB microtubes, (d) anthracene−TCNB microtubes, and (f) microdumbbells comprising naphthalene−TCNB microtubes and anthracene−TCNB tips. (c, e, g) TEM images showing a typical single (c) naphthalene−TCNB microtube, (e) anthracene−TCNB microtube, and (g) microdumbbell. The insets in (c) and (e) show SAED patterns of single naphthalene−TCNB and anthracene−TCNB microtubes, respectively.

micrometers. Transmission electron microscopy (TEM) (Figure 1c) further showed that a single microtube had an inner diameter of ∼1.2 $\mu$m and a wall thickness of ∼600 nm. In addition, selected-area electron diffraction (SAED) (Figure 1c inset) showed that the 1D microtubes had a single-crystalline structure growing along the *c* axis (i.e., the [001] direction). Similarly, the simple liquid-phase strategy was also used to synthesize single-crystalline anthracene−TCNB microtubes (Figure 1d,e). Subsequently, to integrate the different organic materials into one unit, we designed a two-step seeded-growth method in which the well-dispersed naphthalene−TCNB microtubes served as seeds to assist the heterogeneous nucleation and growth of anthracene−TCNB complexes onto their ends (Figure 2a). First, a stock solution of naphthalene−TCNB complexes in acetonitrile (10 mM, 2.5 mL) was quickly injected into 10 mL of an 1:3 (v/v) ethanol/water mixture to induce tubular self-assembly. For growth of the anthracene−TCNB tips, the suspension of naphthalene−TCNB seed microtubes was added into a certain amount of anthracene−TCNB complex solution and allowed to stand for 30 min, after which a yellowish suspension was formed.

To prevent the formation of separate microparticles, the concentration of anthracene−TCNB complex solution had to be precisely controlled below the homogeneous nucleation threshold during coassembly by tuning the naphthalene−TCNB/anthracene−TCNB molar ratio (*N*). SEM clearly demonstrated the selective growth of anthracene−TCNB onto the tips of naphthalene−TCNB microstructures at *N* = 50:3, as indicated by the appearance of bright points with enhanced contrast (Figure 1f). TEM (Figure 1g) showed that the tubular morphology of the seed remained unchanged and that anthracene−TCNB microparticles tightly adhered to the tube tips, resulting in a "microdumbbell". The XRD patterns of the pure naphthalene−TCNB microtubes, anthracene−TCNB microtubes, and the microdumbbells (Figure S1 in the Supporting Information)

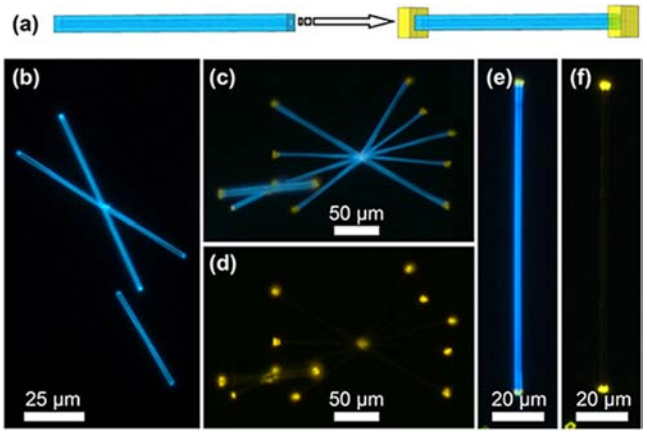


**Figure 2.** (a) Schematic representation of the two-step seeded-growth process: selective nucleation of anthracene−TCNB occurs at the ends of naphthalene−TCNB microtube seeds. (b−f) Fluorescence microscopy images of (b) naphthalene−TCNB microtubes and (c, e) microdumbbells under excitation by nonfocused UV light (330−380 nm) and (d, f) microdumbbells under excitation by blue light (460−490 nm).

agree well with those of the corresponding monoclinic bulk crystals of naphthalene−TCNB and anthracene−TCNB complexes. Moreover, it is worth noting that the addition of anthracene−TCNB did not destroy the original crystal structure of the seed microtubes, and the appearance of a new peak at 11.7° can be indexed to the (110) plane of anthracene−TCNB. This confirms that the anthracene−TCNB microparticles were grown exclusively onto the tips of the existing naphthalene−TCNB microtubes.

Under UV excitation, the crystalline naphthalene−TCNB complex exhibits intense blue emission, whereas crystalline anthracene−TCNB emits intense yellow light (Figure 3a inset).[8] On the basis of their solid-state luminescence features, the microdumbbells consisting of these two distinct CT complexes were examined by fluorescence microscopy (Figure 2b−f). Obviously, under excitation by nonfocused UV light (330−380 nm), pure naphthalene−TCNB microtubes emitted uniform blue photoluminescence (PL) originating from a typical CT transition between the naphthalene electron donor and TCNB electron acceptor (Figure 2b). Meanwhile, pure anthracene−TCNB microtubes exhibited uniform yellow PL when excited by UV light, which become stronger upon irradiation by blue light (Figure S2). In contrast to the single-color-emitting naphthalene−TCNB and anthracene−TCNB microtubes, the microdumbbells appeared as dual-color-emitting heterojunctions, as shown in Figure 2c−f. Remarkably, the naphthalene−TCNB microtube in the middle of each microdumbbell remained blue-emitting when excited by UV light, whereas the anthracene−TCNB microparticles at the tips emitted yellow light. Upon excitation with blue light, the blue-emitting naphthalene−TCNB component became nearly nonemissive, whereas the yellow-emitting tips exhibited strong fluorescence.

To investigate the effect of anthracene−TCNB growth on the optical properties of the seed microtubes, PL measurements were carried out. The PL spectrum of a pure naphthalene−TCNB microtube film spin-coated onto a quartz substrate (Figure 3a, blue curve) shows a broad structureless band at ∼460 nm upon excitation at 365 nm, which arises from a CT transition from the HOMO of naphthalene to the LUMO of TCNB.[8,10] Similarly, the spectrum of an anthracene−TCNB microtube film (Figure 3a, orange curve) shows an emission band at 560 nm upon


dx.doi.org/10.1021/ja3114278 | *J. Am. Chem. Soc.* 2013, 135, 3744−3747

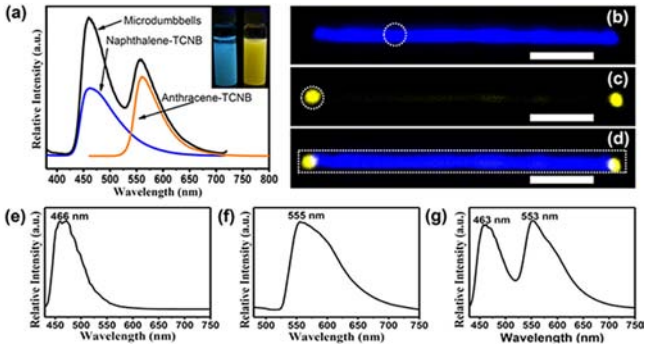


**Figure 3.** (a) PL spectra of naphthalene−TCNB microtubes (blue curve, $\lambda_{ex}$ = 365 nm), anthracene−TCNB microtubes (orange curve, $\lambda_{ex}$ = 460 nm), and microdumbbells (black curve, $\lambda_{ex}$ = 365 nm). The inset shows a photograph of (left) naphthalene−TCNB and (right) anthracene−TCNB microtube suspensions under a UV lamp (365 nm). (b, c) LCFM images of a typical single microdumbbell collected from the (b) blue-light ($\lambda_{ex}$ = 405 nm) and (c) yellow-light ($\lambda_{ex}$ = 458 nm) regions and (d) the dual-color superposed LCFM image. The scale bars correspond to 25 $\mu$m. (e−g) Microarea PL spectra recorded from the selected areas of the microdumbbell marked in white in (b−d).

excitation at 460 nm, corresponding to the typical yellow emission of the anthracene−TCNB complex. The PL spectrum of the microdumbbells consists of a peak at 460 nm due to the naphthalene−TCNB component and another peak at 556 nm due to the anthracene−TCNB component that is slightly blue-shifted from 560 nm. Except for this slight blue shift, the excitation spectra of the microdumbbells at emission bands of (1) 460 nm and (2) 556 nm are consistent with those of naphthalene−TCNB and anthracene−TCNB, respectively (Figure S3). However, the dual-color PL spectrum (Figure 3a, black curve) is not a simple mixture or sum of the individual PL spectra of the component CT complexes because the emission from anthracene−TCNB is so relative to that of naphthalene−TCNB, even though the anthracene−TCNB tips make up only ~6% or less of the total structure. As the solid-state PL efficiencies for naphthalene−TCNB and anthracene−TCNB were measured to be 17.8 and 8.4%, respectively, the relatively intense anthracene−TCNB PL indicates efficient direct energy transfer from naphthalene−TCNB to anthracene−TCNB across the heterojunction interface because of the good overlap of the excitation spectrum of anthracene−TCNB with the emission spectrum of naphthalene−TCNB, similar to the case of organic heterojunctions composed of aluminum tris(8-hydroxyquinoline) trunks and 1,5-diaminoanthraquinone branches.[11]

Further structural characterization of a single microdumbbell comprising naphthalene−TCNB and anthracene−TCNB was performed by color mapping through laser confocal fluorescence microscopy (LCFM). LCFM images of a single typical microdumbbell excited at two different laser wavelengths (Figure 3b−d) and the corresponding PL spectra (Figure 3e−g) clearly revealed the spatial distribution of naphthalene−TCNB and anthracene−TCNB. In particular, a single microdumbbell excited by a 405 nm laser and monitored in the blue-light region (415−500 nm) showed only a blue-emitting segment on the microdumbbell body (Figure 3b). The corresponding microarea PL spectrum (Figure 3e) of the blue-emitting segment (dashed circle in b) shows a single peak at 466 nm due to the characteristic PL of naphthalene−TCNB complexes. The same microdumbbell excited by a 458 nm laser and monitored in the yellow-light region (520−600 nm) showed clear emission of bright yellow light from the two microdumbbell tips, whereas the blue-emitting body was nearly nonemissive (Figure 3c). Moreover, the microarea PL spectrum (Figure 3f) of the tip (dashed circle in c) shows a band at 555 nm, consistent with the PL of anthracene−TCNB complexes. The superposed LCFM image (Figure 3d) also confirms the selective growth of anthracene−TCNB onto the two tips of the naphthalene−TCNB microtube. The PL spectrum of the single microdumbbell (Figure 3g) shows that the intensities of the fluorescence from the seed and the tips are about equal upon excitation at 405 nm, which also indicates that efficient direct energy transfer may be involved in our present system.

To demonstrate further the efficacy of the two-step seeded-growth process, we similarly used this method to synthesize other dumbbell-like heterogeneous microstructures of CT complexes simply by replacing the yellow-emitting anthracene−TCNB with complexes that emit different colors, such as phenanthrene−TCNB (Figure S4) and fluorene−TCNB (Figure S5). As expected, similar to the selective deposition of anthracene−TCNB domains, the simple solution strategy resulted in heterogeneous nucleation of phenanthrene−TCNB or fluorene−TCNB exclusively onto the tips of the naphthalene−TCNB microtube seeds (Figure 4a−d). Moreover,

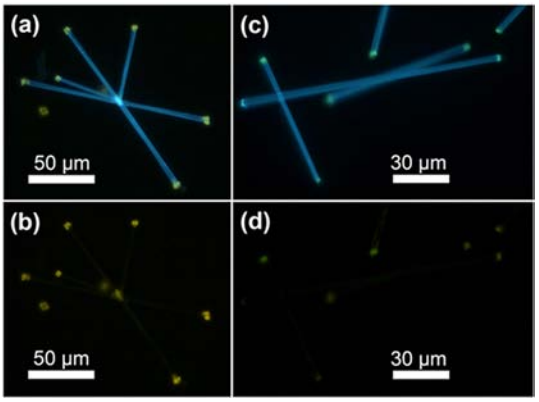


**Figure 4.** Fluorescence microscopy images of microdumbbells composed of naphthalene−TCNB microtubes and (a, b) phenanthrene−TCNB tips or (c, d) fluorene−TCNB tips upon excitation with (a, c) UV light and (b, d) blue light.

phenanthrene−TCNB domains emitted yellow-green light and the fluorene−TCNB emitted green light upon UV excitation of the microdumbbells. The phenanthrene−TCNB component turned into yellow light while the green fluorene−TCNB emission became weaker under blue-light excitation.

The mechanism for the selective growth of anthracene−TCNB onto the ends of naphthalene−TCNB microtubes was elucidated through structural analysis of the two crystals and surface−interface energy balance.[12,13] As reported previously,[9] the two-component molecules are nearly planar in the naphthalene−TCNB and anthracene−TCNB complexes and are stacked alternately along the *c* axis. Hence, only the end facets of single-crystalline naphthalene−TCNB microtubes have exposed TCNB molecules, which would induce the selective nucleation of anthracene−TCNB because of the strong CT interaction between the anthracene donor and the TCNB acceptor. The unit cells of the two crystals have similar *a* and *b* lattice parameters and significantly different lattice parameters along the *c* axis (*a* = 9.39 Å, *b* = 12.66 Å, *c* = 6.87 Å for naphthalene−TCNB and *a* = 9.505 Å, *b* = 12.748 Å, *c* = 7.417 Å


dx.doi.org/10.1021/ja3114278 | J. Am. Chem. Soc. 2013, 135, 3744−3747

for anthracene−TCNB), so formation of a continuous, uniform core−shell geometry would be difficult. Consequently, the large mismatch in the *c* parameter versus the small lattice mismatch of the (001) surface of naphthalene−TCNB and anthracene−TCNB (Figure S6) preferentially favors the anisotropic growth of anthracene−TCNB onto the tips of the seed crystal along the *c* axis. On the other hand, surface−interface energy balance considerations would also prefer anthracene−TCNB nucleation at the end facets, because it would eliminate the unstable or high-energy naphthalene−TCNB facets, as in the case of b-$TiO_2$−$Fe_xO_y$ nanorod heterostructures.[13] Nevertheless, the growth of anthracene−TCNB on the side surface of naphthalene−TCNB microtubes became feasible when *N* for the two-step seeded-growth process was changed from 50:3 to 50:6 (Figures S7c−d and S9). Meanwhile, it is apparent that surface defects would also induce the growth of anthracene−TCNB on the defect sites (Figures S7d and S10). Indeed, selective growth of phenanthrene−TCNB onto the tips of naphthalene−TCNB microtubes can serve as another example to support the above growth mechanism. As reported previously,[14] a homogeneous mixed molecular crystal made of phenanthrene−TCNB and anthracene−TCNB complexes can form over the whole composition range [$(anthracene)_{1-x}(phenanthrene)_x$−TCNB], analogous to a solid solution. Considering the small lattice mismatch between the phenanthrene−TCNB ($a$ = 9.413 Å, $b$ = 13.104 Å, $c$ = 7.260 Å) and anthracene−TCNB complexes, anthracene−TCNB can be replaced successfully by phenanthrene−TCNB to form dumbbell-like architectures with naphthalene−TCNB seed microtubes.

In summary, we have introduced a simple two-step seeded-growth process for fabricating dual-color-emitting heterogeneous microdumbbells comprising two distinct color-emitting domains made of luminescent organic CT complexes. This process exploits the selective and anisotropic growth of one organic CT complex onto the ends of a microtube of another organic CT complex acting as a seed. In principle, by a judicious choice of organic CT complexes, the present growth process could be used to fabricate a wide range of sophisticated dual- or multicolor-emitting heterojunction microdumbbells. Such lab-on-a-particle architectures that provide a simple route for integration of dissimilar organic materials would have myriad applications in miniaturized devices, such as multicolor fluorescent barcodes and optical switches. Furthermore, the heterojunction microstructures provide a promising platform for investigating selective and anisotropic nucleation and growth of organic CT complexes. Specifically, the simple two-step solution seeded-growth strategy may be extended to organic semiconductors with similar structural properties in order to access p−n heterojunction micro- and nanostructures with desirable spatial organization of different materials.

## ■ ASSOCIATED CONTENT

### Supporting Information

Detailed experimental procedures, XRD patterns and additional SEM and fluorescence microscopy images of dual-color-emitting microdumbbells, and SEM images and PL spectra of phenanthrene−TCNB and fluorene−TCNB microtubes. This material is available free of charge via the Internet at http://pubs.acs.org.

## ■ AUTHOR INFORMATION

### Corresponding Author

lsliao@suda.edu.cn; apannale@suda.edu.cn

### Notes

The authors declare no competing financial interest.

## ■ ACKNOWLEDGMENTS

This work was supported by the National Natural Science Foundation of China (61036009, 61177016, and 21161160446), The National 863 Project of China (2011AA03A110), the Natural Science Foundation of Jiangsu Province (BK2010003), and the National Basic Research Program of China (973 Program) (2009CB623703). This work was also funded by Priority Academic Program Development of Jiangsu Higher Education Institutions (PAPD). The authors thank F. Peng for assistance with collecting the LCFM data.

## ■ REFERENCES

(1) (a) Milliron, D. J.; Hughes, S. M.; Cui, Y.; Manna, L.; Li, J. B.; Wang, L. W.; Alivisatos, A. P. *Nature* **2004**, *430*, 190. (b) Wang, W. S.; Goebl, J.; He, L.; Aloni, S.; Hu, Y. X.; Zhen, L.; Yin, Y. D. *J. Am. Chem. Soc.* **2010**, *132*, 17316. (c) Sadtler, B.; Demchenko, D. O.; Zheng, H. M.; Hughes, S. M.; Merkle, M. G.; Dahmen, U.; Wang, L. W.; Alivisatos, A. P. *J. Am. Chem. Soc.* **2009**, *131*, 5285. (d) Habas, S. E.; Yang, P. D.; Mokari, T. *J. Am. Chem. Soc.* **2008**, *130*, 3294. (e) Buck, M. R.; Bondi, J. F.; Schaak, R. E. *Nat. Chem.* **2012**, *4*, 37. (f) Mokari, T.; Sztrum, C. G.; Salant, A.; Rabani, E.; Banin, U. *Nat. Mater.* **2005**, *4*, 855. (g) Pacholski, C.; Kornowski, A.; Weller, H. *Angew. Chem., Int. Ed.* **2004**, *43*, 4774. (h) Kudera, S.; Carbone, L.; Casula, M. F.; Cinglolani, R.; Falqui, A.; Snoeck, E.; Parak, W. J.; Manna, L. *Nano Lett.* **2005**, *5*, 445.

(2) Mokari, T.; Rothenberg, E.; Popov, I.; Costi, R.; Banin, U. *Science* **2004**, *304*, 1787.

(3) (a) Yu, H.; Chen, M.; Rice, P. M.; Wang, S. X.; White, R. L.; Sun, S. H. *Nano Lett.* **2005**, *5*, 379. (b) Wang, C.; Xu, C. J.; Zeng, H.; Sun, S. H. *Adv. Mater.* **2009**, *21*, 3045. (c) Li, X. H.; Lian, J.; Lin, M.; Chan, Y. T. *J. Am. Chem. Soc.* **2011**, *133*, 672. (d) Deka, S.; Falqui, A.; Bertoni, G.; Sangregorio, C.; Poneti, G.; Morello, G.; De Giorgi, M.; Giannini, C.; Cingolani, R.; Manna, L.; Cozzoli, P. D. *J. Am. Chem. Soc.* **2009**, *131*, 12817. (e) Casavola, M.; Grillo, V.; Carlino, E.; Giannini, C.; Gozzo, F.; Pinel, E. F.; Garcia, M. A.; Manna, L.; Cingolani, R.; Cozzolli, P. D. *Nano Lett.* **2007**, *7*, 1386.

(4) (a) Gu, H. W.; Yang, Z. M.; Gao, J. H.; Chang, C. K.; Xu, B. *J. Am. Chem. Soc.* **2005**, *127*, 34. (b) Selvan, S. T.; Patra, P. K.; Ang, C. Y.; Ying, J. Y. *Angew. Chem., Int. Ed.* **2007**, *46*, 2448. (c) Choi, J.; Jun, Y.; Yeon, S. I.; Kim, H. C.; Shin, J. S.; Cheon, J. *J. Am. Chem. Soc.* **2006**, *128*, 18982.

(5) (a) Costi, R.; Saunders, A. E.; Elmalem, E.; Salant, A.; Banin, U. *Nano Lett.* **2008**, *8*, 637. (b) Li, P.; Wei, Z.; Wu, T.; Peng, Q.; Li, Y. D. *J. Am. Chem. Soc.* **2011**, *133*, 5660. (c) Shemesh, Y.; Macdonald, J. E.; Menagen, G.; Banin, U. *Angew. Chem., Int. Ed.* **2011**, *50*, 1185.

(6) Zhang, W.; Jing, W. S.; Fukushima, T.; Saeki, A.; Seki, S.; Aida, T. *Science* **2011**, *334*, 340.

(7) Zhang, Y. J.; Dong, H. L.; Tang, Q. X.; Ferdous, S.; Liu, F.; Hu, W. P.; Briseno, A. L. *J. Am. Chem. Soc.* **2010**, *132*, 11580.

(8) Mataga, N.; Murata, Y. *J. Am. Chem. Soc.* **1969**, *91*, 3144.

(9) Lei, Y. L.; Jin, Y.; Zhou, D. Y.; Gu, W.; Shi, X. B.; Liao, L. S.; Lee, S. T. *Adv. Mater.* **2012**, *24*, 5345.

(10) Iwata, S.; Tanaka, J.; Nagakura, S. *J. Am. Chem. Soc.* **1967**, *89*, 2813.

(11) Zhen, J. Y.; Yan, Y. L.; Wang, X. P.; Zhao, Y. S.; Huang, J. X.; Yao, J. N. *J. Am. Chem. Soc.* **2012**, *134*, 2880.

(12) Carbonea, L.; Cozzolia, P. D. *Nano Today* **2010**, *5*, 449.

(13) Buonsanti, R.; Grillo, V.; Carlino, E.; Giannini, C.; Gozzo, F.; Garcia-Hernandez, M.; Garcia, M. A.; Cingolani, R.; Cozzoli, P. D. *J. Am. Chem. Soc.* **2010**, *132*, 2437.

(14) Wright, J. D.; Ohta, T.; Kuroda, H. *Bull. Chem. Soc. Jpn.* **1976**, *49*, 2961.